ACCEPTED MANUSCRIPT

In vitro assessment of the differences in retinal ganglion cell responses to intra- and extracellular electrical stimulation

To cite this article before publication: Rebecca Kotsakidis *et al* 2018 *J. Neural Eng.* in press https://doi.org/10.1088/1741-2552/aac2f7

In vitro assessment of the differences in retinal ganglion cell responses to intra- and extracellular electrical stimulation

Rebecca Kotsakidis[1], Hamish Meffin[1,2],
Michael R Ibbotson[1,2], Tatiana Kameneva[3,4] *

Abstract

Objective To compare responses of retinal ganglion cells (RGCs) to intracellular and extracellular electrical stimulation of varying frequency and amplitude. **Approach** *In vitro* patch clamp was used to record the responses of RGCs to sinusoidal current stimulation of varying frequency and amplitude. The results were simulated using the Neuron software package. **Main results** The stimulation frequency yielding the greatest response was higher for extracellular stimulation compared to intracellular stimulation in the same cells (256 Hz versus 64 Hz). In fact, at the high end of the frequency range, where extracellular stimulation was highly efficacious, no responses could be generated using intracellular stimulation. A region in the amplitude-frequency stimulation space was identified where OFF-RGCs could be preferentially stimulated over ON-RGCs. We found that the inability of RGCs to respond at high frequencies of intracellular stimulation is likely the result of the axon acting as a low pass filter. **Significance** There is no direct translation of the results obtained with intracellular stimulation to those that employ extracellular stimulation.

1   Introduction

Electrical stimulation of neural tissue has been used in neural prostheses, and also as a research tool [2], [3], [12], [16], [20], [21], [24]. Despite a large body of published work exploring the fundamental mechanisms governing the responses of neurons to electrical stimulation [5], [21], it is not clear how results obtained with intracellular stimulation would inform the stimulation parameters required to excite neural tissue using extracellular stimulation. Extracellular stimulation is a classical technique used in neuroprosthetics [3], [20], while intracellular stimulation is often used during *in vitro* experiments to study the responses of individual neurons to stimulation [16].

*[1]National Vision Research Institute, Australian College of Optometry, Australia. [2]Department of Optometry and Vision Sciences, University of Melbourne, Australia. [3]Faculty of Science, Engineering and Technology, Swinburne University of Technology, Australia. [4]Department of Biomedical Engineering, The University of Melbourne, Australia. Contact: Tatiana Kameneva, tkameneva@swin.edu.au

Experiments conducted *in vitro* make it possible to study neural responses under more carefully controlled and easily manipulated situations than *in vivo* experiments or clinical studies. It is often assumed that results obtained *in vitro* using intracellular stimulation directly translate to the *in vivo* setting and in the clinic (where extracellular stimulation is used). However, no comprehensive study in the retina has been done to date that compares responses to intracellular and extracellular stimulation in the same cell. We address this issue by comparing responses of retinal ganglion cells (RGCs) to sinusoidal stimulation with intracellular and extracellular electrodes at a range of frequencies and amplitudes. Sinusoidal stimulation has been extensively used in neuroscience to study the responses of neurons to electrical stimulation [28], [9]; for comparative purposes, this is the stimulation paradigm used here.

RGCs are the output neurons of the retina that transmit information to the visual cortex via the optic nerve. RGCs can be divided into ON, OFF, and ON-OFF cell types based on their responses to light and their dendritic tree stratification in the inner plexiform layer of the retina. ON cells respond with higher spike rates when light is presented to the center of their receptive fields, while OFF cells respond most strongly after light offset. ON-OFF type cells respond to both, light onset and light offset. While ON and OFF cells respond to opposite brightness polarities, both cell types are stimulated simultaneously with electrical stimulation via the multielectrode arrays used in retinal neuroprosthetic implants. Thus, the response to electrical stimulation is very different to natural stimulation, and may cause cancelation of signals in higher visual centers of the cortex. In this work, we explored the possibility of differentially stimulating ON and OFF RGCs by comparing cell responses to sinusoidal stimulation of varying frequencies and amplitudes in the two cell types.

To compare responses of RGCs to intracellular and extracellular stimulation, we applied sinusoidal waveforms of varying frequency and amplitude. We found clear differences in the preferred frequencies of stimulation between intracellular and extracellular stimulation. The optimal stimulation frequency required to elicit maximum responses was different for intra- and extracellular stimulation. While cells responded to high frequency extracellular stimulation, no increase in spiking was observed for high frequency intracellular stimulation even at higher amplitudes of stimulation. We found a region in the amplitude-frequency stimulation space where OFF-RGCs can be preferentially stimulated over ON-RGCs. Using Hodgkin-Huxley models and morphologically correct models of RGCs simulated using Neuron, we suggest that the inability of cells to follow high frequency intracellular stimulation may be due to the axon acting as a low pass filter.

2   Methods

2.1   Experiments

Experiments were conducted at the National Vision Research Institute, Australian College of Optometry. All protocols conformed to the policies of the National Health and Medical Research Council of Australia and were approved by the Animal Experimentation Ethics Committee of the University of Melbourne.

2

Retinal Dissection

Data were collected from healthy mice (C57BL/6) whose age varied between 57 to 81 days. The mice were weighed to determine the volume of required anaesthetics. A mixture of Ketamine (0.135ml/100g) and Xylazine (0.08ml/100g) was used to anaesthetize the animals. The mice were checked for muscle reflexes and pupil responses before the surgery to ensure the mouse was non-respondent. Both eyes were removed. On each side of the eye the sclera was pierced and the cornea and lens removed to ensure the health of the retina was maintained. The vitreous humour was removed with micro tweezers under a dissecting microscope (Zeiss, Germany). The retina was carefully separated from the pigment epithelium by peeling it slowly off the retina. The retinae were perfused with carboxygen at a flow of 3-5 ml/min with an extracellular solution consisting of 30 g of AMES medium (Sigma-Aldrich, St, Louis, MO), 1.900 g of D-(+)-glucose and 1.8 g of sodium bicarbonate. The temperature of the chamber ranged between 19 and 24 °C. The experimental setup is illustrated in Figure 1.A. The retinal tissue was mounted onto a 2.2 x 4 cm stage and held down by magnets (Fig. 1.C). The tissue sample was mounted onto a glass slide, photoreceptor side down, and covered with a plastic stage containing a stainless steel metal harp with fine horizontal strings made of Lycra threads (Warner Instruments, CT, USA), as illustrated in Figure 1.B.

Patch-clamp Recording

The retina was viewed under an upright microscope (BX51WI, Olympus, Shinjuku, Japan) fitted with a 40x water immersion lens and a CCD camera (Ikegami, ICD-48E). Glass filaments of size 1.5mm x 0.86mm (A-M systems, WA, Australia) were made into micro pipettes using a Flaming/Brown Micropipette Puller (P-97, Sutter Instrument Company, Novato, CA, USA). Rip pipettes (4-9 MΩ) were used to make small holes in the inner limiting membrane to expose cells (Fig. 1D). Patching pipettes were filled with an internal solution composed of 9 μl K-glutamate, 5 μl Energy Cache, and 2.5 μl of biocytin and 2.5 μl of Alexa Hydrazide 488 dye. Whole cell current-clamp recordings were obtained following standard procedures [10].

The patch electrode was placed just off-center on the cell body and slowly lowered (Fig. 1.E). When a dimple was seen above the cell, negative pressure was applied using a 1ml syringe to create suction in the pipette, such that the -15 pA pulses appeared on the computer stimulation interface.

The return electrode was made from silver wire with a diameter of 0.375 mm. The tip of the wire was melted to produce a spherical shape with a diameter of 1.5 mm. An Ag/AgCl electrode was then formed by electrolysis in potassium chloride.

Electrical Stimulation

The intracellular patch electrode administered stimulation through the internal solution to the pipette tip. The intracellular patch electrode and ground electrodes were composed of silver and coated with silver chloride before each experiment. Sinusoidal currents of the stipulated amplitude were administered through the internal solution to the pipette tip in
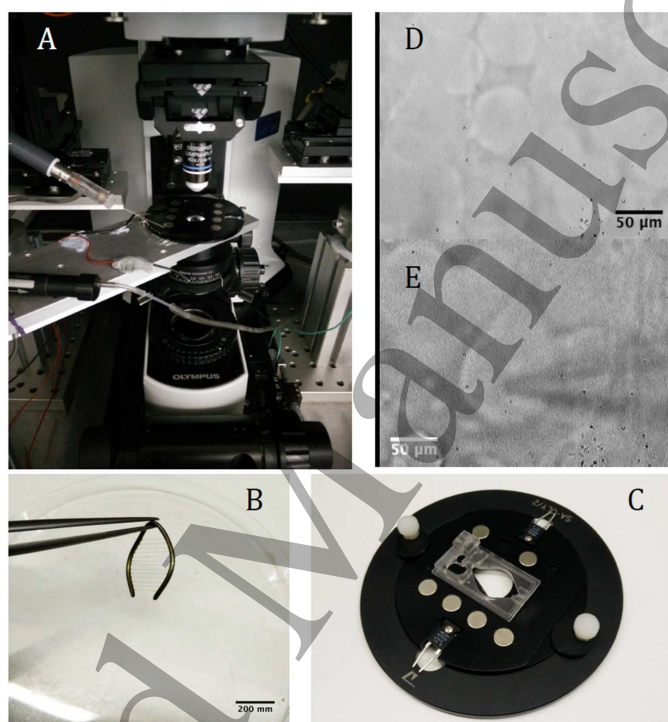
Fig. 1: Experimental setup. A. An Olympus upright microscope with 40x objective was used to view the retina. In front are plastic tubes used to perfuse the extracellular solution into the retina. B. The harp used to hold down the retina made of fine lycra strings. C. The stage in which the retina is mounted. The clear plastic chamber contains the retina and is held down by magnets (not shown). D. A hole is made in the inner limiting membrane to expose the ganglion cells below. E. A pipette of 5-11 MΩ is lowered onto a cell using a micromanipulator to make a dimple.

4
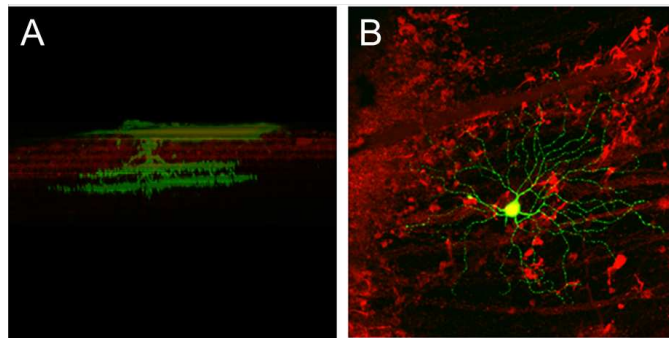
Fig. 2: Examples of imaged cells. A. The bi-stratification of an ON-OFF cell in the inner plexiform layer is shown in green. B. ON cell with radial arrangement of dendrites and large cell body.

the case of intracellular stimulation, or through a Pt electrode in the case of extracellular stimulation.

The extracellular stimulating electrode was placed above the inner limiting membrane during extracellular experiments and approximately 100-200 μm from the cell being patched. The extracellular stimulation experiments were performed with a large diameter, 0.5 mm, platinum stimulation electrode.

The return electrode was positioned approximately 2.5 mm from the stimulating electrode.

Cells were stimulated with intracellular and extracellular sinusoidal current of varying amplitudes and frequencies and their responses were analyzed. Tested stimulation frequencies were in the range of 2 to 2048 Hz for both intracellular and extracellular protocols, i.e. 2, 4, 8, 16, 32, 64, 128, 256, 512, 1024, 2048 Hz. Logarithmic steps were used to allow coverage of a wide range of frequencies. Tested amplitudes were between 1 and 905 pA for the intracellular stimulation and 1 to 256 μA for the extracellular stimulation. In all cases, a logarithmic (doubling) step size was used.

Combinations of stimulation with varying amplitudes and frequencies were delivered in a randomized order and each combination was repeated 2 to 8 times, depending on the health of the cell.

Cell classification

Cells were classified into ON, OFF, and ON-OFF classes based on their light responses and the dendritic stratification following standard procedures [25]. Cells were classified according to their dendritic size, cell body size and dendrite stratification among other factors. An Olympus confocal microscope with water immersion lenses of x20 and x40 was used. Examples of imaged cells are illustrated in Figure 2.

Data analysis

A custom-made MATLAB interface (MathWorks, R2014a) was used to command a multi-channel stimulator (Tucker Davis Technologies) and send different waveform signals for stimulation. Data was collected using National Instruments LabView software.
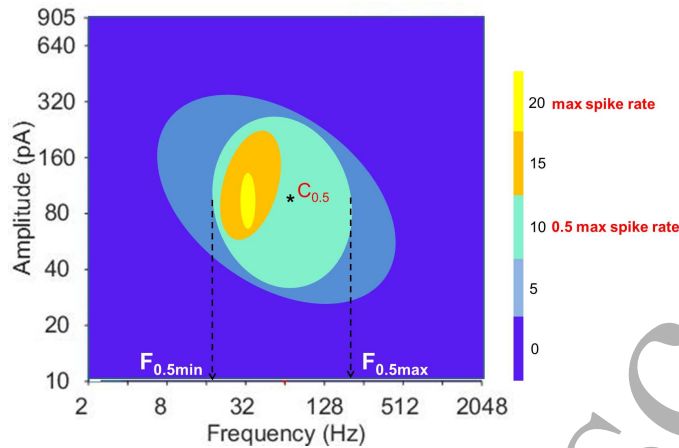
Fig. 3: A cartoon of a contour map showing the number of spikes per second in response to electrical stimulation. The colorbar indicates the maximum spike rate in yellow (20 Hz) making the half spike rate at the green level of 10 Hz. At the half spike rate, the maximum ($F_{0.5max}$) and minimum ($F_{0.5min}$) frequencies, the center of frequency stimulation ($C_{0.5}$) and the frequency bandwidth (B_F) were calculated along the horizontal axis. The amplitude bandwidth (B_A) was also calculated along the vertical axis of the contour map.

To compare cell responses to the intracellular and extracellular stimulation of varying frequency and amplitude, a contour map was used. The contour map plotted a spike rate for combinations of stimulation amplitudes and frequencies. A comparison was made for individual cells (intracellular vs extracellular responses) and for populations of cells. In addition, responses between ON, OFF and ON-OFF classes were compared and analyzed.

For each cell, the center frequency of the region at half the maximum spike rate was calculated ($C_{0.5}$ in Figure 3). The minimum and maximum stimulation frequencies of contour activation at half the spike rate were calculated ($F_{0.5min}$ and $F_{0.5max}$ in Figure 3), and the stimulation frequency bandwidth in octaves was calculated for each cell, i.e. $B_F = \log_2(F_{0.5max}/F_{0.5min})$. The stimulation amplitude bandwidth was calculated similarly, $B_A = \log_2(A_{0.5max}/A_{0.5min})$. The values for $C_{0.5}$, B_F and B_A were compared between intracellular and extracellular stimulation for all cells.

2.2 Computer Simulations

A multiple-compartment model was used to explore the mechanisms behind different RGC responses to intracellular and extracellular stimulation. The cell morphology was exported from the NeuroMorpho database [1]. A medium size complex cell CTT1209A was simulated (the cell morphology is shown in Figure 4). The axon was modelled using three regions: the initial segment, narrow segment and distal axon. The distal axon had a diameter of 1 μm and a length of 5340 μm. Hodgkin-Huxley models were simulated in the NEURON environment [11]. The backward Euler method was used in simulations with a time step size of 0.01 ms. Simulations were run with the temperature at 22 ^{o}C. Simulation results were analyzed in MATLAB (MathWorks, R2016a).

Kirchoff's law described the dynamics of the membrane potential, V_m. Leak, sodium,

6

A

B
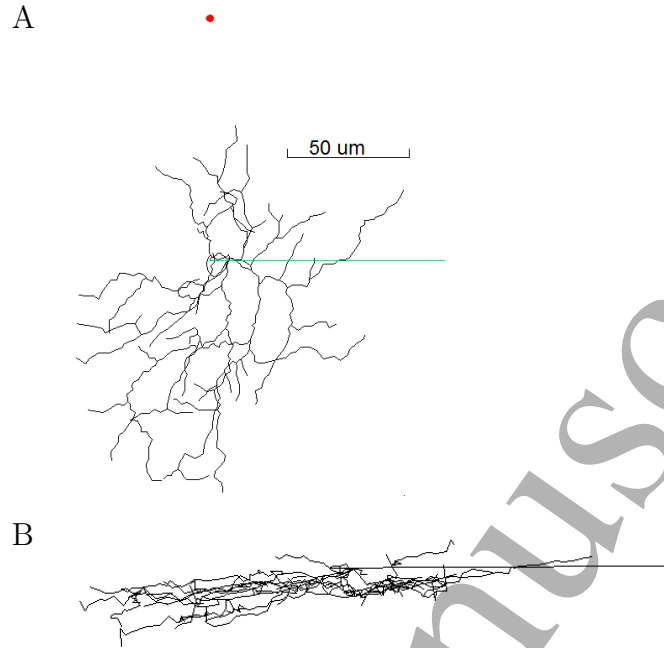
Fig. 4: A. Morphology of the simulated cell. The red circle (above) shows the location of the extracellular stimulating electrode. The axon is indicated by the green line. The left hand tip of the horizontal green line indicates the exit point of the axon. B. The same neuron, rotated.

calcium and potassium currents were summed according to the following,

$$C_{\mathrm{m}}\frac{dV}{dt} = \bar{g}_{\mathrm{L}}(V - V_{\mathrm{L}}) + \bar{g}_{\mathrm{Na}}m^3h(V - V_{\mathrm{Na}}) + \bar{g}_{\mathrm{Ca}}c^3(V - V_{\mathrm{Ca}})$$

$$+ (\bar{g}_{\mathrm{K}}n^4 + \bar{g}_{\mathrm{K,A}}p^3q + \bar{g}_{\mathrm{K(Ca)}})(V - V_{\mathrm{K}}) + I_{\mathrm{stim}}, \tag{1}$$

where C_{m} is the specific capacitance of the membrane, $\bar{g}$ is the maximum conductance of an ionic current, and m, h, c, n, p, q are gating variables of the voltage-gated currents. Gating variables were described by first-order kinetic equations as in [6],

$$\frac{dx}{dt} = -(\alpha_x + \beta_x)x + \alpha_x. \tag{2}$$

Variables α_{x} and β_{x} are given in Table 1. Values of conductances in different compartments of the model are given in Table 2.

Leak, sodium, calcium, delayed rectifier potassium, A-type, and Ca-activated potassium currents had dynamics as described in [6]. The value of reversal potentials for leak, sodium, and potassium current were fixed: $V_{\mathrm{Na}} = 35$ mV, $V_{\mathrm{K}} = -75$ mV, $V_{\mathrm{L}} = -62$ mV. The value of the reversal potential for the calcium current varied with time,

$$V_{\mathrm{Ca}}(t) = \frac{RT}{2F} \ln\left(\frac{[\mathrm{Ca}^{2+}]_{\mathrm{e}}}{[\mathrm{Ca}^{2+}]_{\mathrm{i}}(t)}\right), \tag{3}$$

where $R = 8.314$ J/(M·K) is the gas constant, T is temperature in Kelvin, $F = 9.684 \cdot 10^4$ C/M is the Faraday constant, $[\mathrm{Ca}^{2+}]_{\mathrm{e}} = 1.8$ mM is the extracellular calcium ion

concentration, and $[\text{Ca}^{2+}]_i$ is the intracellular calcium ion concentration such that,

$$\frac{d[\text{Ca}^{2+}]_i(t)}{dt} = \frac{-3I_{\text{Ca}}(t)}{2Fr} - \frac{[\text{Ca}^{2+}]_i(t) - [\text{Ca}^{2+}]_{\text{res}}}{\tau_{\text{Ca}}}, \tag{4}$$

$r = 0.1$ um is the depth of the calcium pump beneath the membrane and $\tau_{\text{Ca}} = 1.5$ ms is the time constant for the intracellular calcium concentration. $[\text{Ca}^{2+}]_{\text{res}} = 10^{-4}$ mM is the residual level above which the free intracellular calcium ions are removed from the cell.

For simulations with intracellular stimulation, I_{stim} was set to the amplitude of the intracellular stimulation current. The intracellular current was injected directly into the center of the soma.

For simulations with extracellular stimulation, the effect of the extracellular potential was taken into account for each segment in the multicompartment model. The extracellular medium was assumed to be homogeneous. An extracellular point electrode was positioned 100 μm above the center of the soma. The extracellular potential, V_{ext}, produced by the extracellular stimulation current I_{stim} was calculated according to the following,

$$V_{\text{ext}}(x, y, z) = Z_{\text{ext}}(x, y, z)I_{\text{stim}}, \tag{5}$$

where Z_{ext} is a transfer impedance and (x, y, z) are cartesian coordinates. The transfer impedance was calculated according to

$$Z_{\text{ext}}(x, y, z) = \frac{\rho}{4\pi r}, \tag{6}$$

where $\rho = 35.4\Omega cm$ is the resistivity of the tissue. To approximate the resistivity of the tissue, the value for a squid axon cytoplasm was used in simulations. This value is lower than the resistivity of mammalian brain or retina tissue; however, this should not affect our qualitative results and conclusions. For a comparison of the values published in the literature for the conductivity of brain tissues in different animals for *in vitro* and *in vivo* experiments, refer to [15]. $r = \sqrt{(x - x_e)^2 + (y - y_e)^2 + (z - z_e)^2}$, (x_e, y_e, z_e) is the location of the stimulation electrode. We assume that the extracellular space is conductive, linear and purely resistive. We assume that the neuron's electrical activity does not have any effect on the extracellular stimulating field. V_{ext} was calculated for all points in space and applied at all compartments of the model.

Sinusoidal stimulation of varying amplitude and frequency was applied. Responses in the soma and in the axon were compared when the intracellular stimulation and extracellular stimulation were applied. The amplitude of subthreshold oscillations in the soma and in the axon were analyzed to verify that the axon acts as a low-pass filter and the number of spikes in response to intra- and extracellular stimulation were recorded.

8

Table 1. Gating parameters for voltage-gated ion channels, [6].

Na$^+$ channel	$\alpha_m = \frac{-0.6(V+30)}{e^{-0.1(V+30)}-1}$ $\alpha_h = 0.4e^{-(V+50)/20}$	$\beta_m = 20e^{-(V+55)/18}$ $\beta_h = \frac{6}{1+e^{-0.1(V+20)}}$
Ca^{2+} channel	$\alpha_c = \frac{-0.3(V+13)}{e^{-0.1(V+13)}-1}$	$\beta_c = 10e^{-(V+38)/18}$
K$^+$ channel	$\alpha_n = \frac{-0.02(V+40)}{e^{-0.1(V+40)}-1}$	$\beta_n = 0.4e^{-(V+50)/80}$
K$_\mathrm{A}^+$ channel	$\alpha_p = \frac{-0.006(V+90)}{e^{-0.1(V+90)}-1}$ $\alpha_q = 0.04e^{-(V+70)/20}$	$\beta_p = 0.1e^{-(V+30)/10}$ $\beta_q = \frac{0.6}{1+e^{-0.1(V+40)}}$

Table 2. Conductance values used in the simulations, [S/cm^2], [6].

	Soma	Dendrites	In.segm.	Narr.segm.	Axon
$\bar{g}_\mathrm{L}$	8×10^{-6}	8×10^{-6}	8×10^{-6}	8×10^{-6}	8×10^{-6}
$\bar{g}_\mathrm{Na}$	0.08	0.025	0.15	0.2	0.07
$\bar{g}_\mathrm{Ca}$	0.0015	0.002	0.0015	0	0
$\bar{g}_\mathrm{K}$	0.018	0.012	0.018	0.018	0.018
$\bar{g}_\mathrm{K,A}$	0.054	0.036	0.054	0	0
$\bar{g}_\mathrm{K(Ca)}$	6.5×10^{-5}	10^{-6}	6.5×10^{-5}	6.5×10^{-5}	6.5×10^{-5}

3 RESULTS

3.1 Experiments

Representative cell membrane potential traces from one cell in response to intracellular and extracellular stimulation are shown in Figure 5. The top row for each frequency of stimulation illustrates the cell's response to intracellular stimulation, while the bottom row shows the membrane potential traces during extracellular stimulation. Three responses are shown for each frequency: low amplitude stimulation (left column, 20 pA for intracellular and 4 uA for extracellular), medium amplitude stimulation (middle column, 80 pA for intracellular and 16 uA for extracellular), and high amplitude stimulation (right column, 320 pA for intracellular and 32 uA for extracellular). The x-axis shows the time interval of stimulation (1 second, between ticks) with 0.1 seconds with no stimulation shown prior to and after the ticks. The results show that the cell responses are suppressed when stimulated at high frequency. However, the number of spikes in response to extracellular stimulation is higher compared to intracellular stimulation.

Individual cell comparisons in response to intracellular and extracellular stimulation are shown in Figure 6. Similar to the data in Figure 5, the individual responses had similar shifts in the optimal stimulation frequency, i.e. maximum spike rate was observed at higher stimulation frequencies with extracellular stimulation than with intracellular stimulation. The colorbars show the spike rate in response to stimulation. The contour map illustrates that the maximum response (yellow area) occurs at higher frequencies of stimulation for extracellular stimulation than for the intracellular stimulation (the yellow

9

area is shifted right in the right column compared to the plots in the left column). Top row in Figure 6 illustrates the response of the cell shown in Figure 5.

The population response (i.e. summed activity over all recorded RGCs) to varying frequencies and amplitudes of sinusoidal stimulation is shown in Figure 7 as contour maps. There are significant differences between RGC responses to intracellular (left column) and extracellular (right column) stimulation. Similar to the individual cell data in Figure 6, the maximum response occurs at higher frequencies of stimulation for extracellular stimulation than for the intracellular stimulation. On average, RGC peak population responses were recorded at 256 Hz and 32 uA in response to extracellular stimulation and at 64 Hz and 640 pA in response to the intracellular stimulation. The cells responded minimally when high frequency intracellular stimulation was applied. High spike activity at low stimulation amplitudes is mainly due to spontaneous activity.

Some differences in responses were observed between ON and OFF RGCs (e.g. Fig. 7, compare second and third rows, ON vs OFF cells). Figure 8 illustrates the differences in spiking between ON and OFF RGCs (ON rate - OFF rate). Hot areas (red) indicate stimulation frequencies and amplitudes that preferentially stimulated ON cells, cold areas (blue) indicate stimulation frequencies and amplitudes that can be used to preferentially stimulate OFF cells. The analysis was repeated for intracellular (Fig. 8A) and extracellular (Fig. 8B) stimulation.

Statistical analysis of the contour maps is shown in Figure 9. The fraction of cells in the population displaying the characteristics presented for intracellular stimulation (red) and for extracellular stimulation (blue) are shown on the y-axis. The absence of a line for some values (for example, below 4 in subplot A) indicates that there were no cells in the population having these values. Subplot A illustrates the stimulation frequency center point of activation at half spike rate, $C_{0.5}$ (refer to Methods for details). Results showed that the centre of activation at half maximum spike rate was smaller for intracellular stimulation. Most cells had the center points between 128 and 512 Hz for extracellular stimulation, while the spread of center point for intracellular stimulation occurred at the lower frequency of stimulations, 8 - 256 Hz.

The stimulation frequency bandwidth, B_F, is shown in Figure 9B, and the stimulation amplitude bandwidth, B_A, is shown in Figure 9C. There are clear differences in the stimulation frequency and amplitude bandwidths for the contour activation at half maximum spike rate between the responses to intracellular and extracellular stimulation. The same data that is presented in Figure 9A-C are shown in Figure 9D-F as scatter plots to appreciate the variability between cells.

3.2   Computer Simulations

Simulated membrane potentials in response to intracellular and extracellular stimulation of varying frequencies are shown in Figure 10. The illustrated frequencies of stimulation are the same as in Figure 5 for experimental data (16, 64, 256 and 1024 Hz). The amplitudes of stimulation (200 pA intracellular and 170 μA extracellular) were chosen to elicit a similar number of spikes in response to intra- and extracellular stimulation at 64 Hz and similar amplitudes of subthreshold oscillations in the soma and axon in response to intra- and extracellular stimulation at 64 Hz. Simulation results showed that with

10

A. Stim Frequency 16 Hz
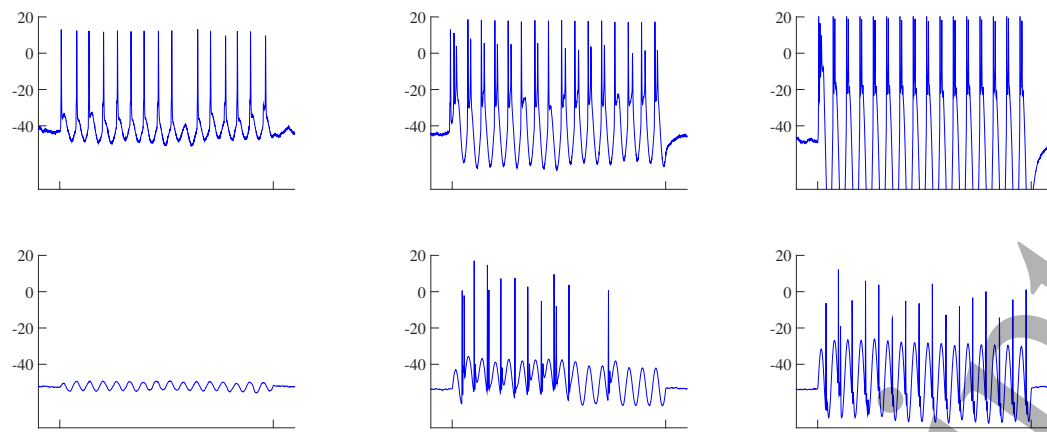
B. Stim Frequency 64 Hz
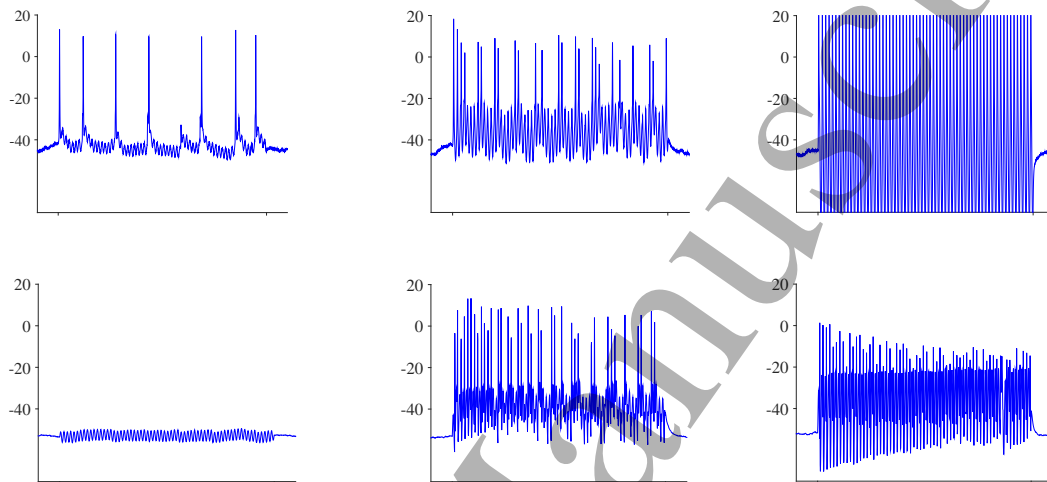
C. Stim Frequency 256 Hz
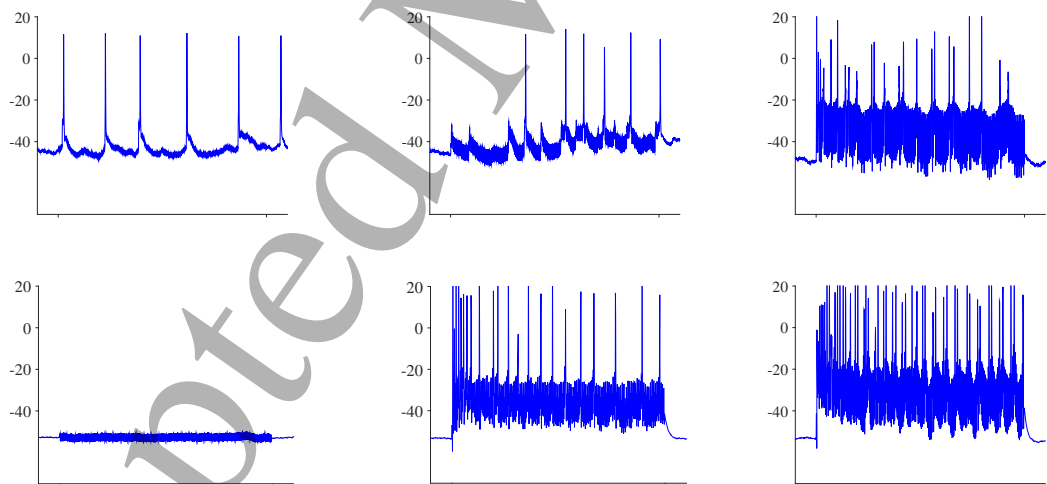
Stim Amp: Low   Medium   High

Fig. 5: Membrane potential traces from one cell in response to intracellular and extracellular stimulation. A. Response of the cell to 16 Hz stimulation. B. Response of the cell to 64 Hz stimulation. C. Response of the cell to 256 Hz stimulation. For each frequency of stimulation, the top row illustrates responses to intracellular stimulation for low (left column), medium (middle column) and high amplitude (left column). The bottom row illustrates responses to extracellular stimulation. For intracellular stimulation, responses to the following amplitudes are shown: 20, 80, 320 pA. For extracellular stimulation, responses to the following amplitudes are shown: 4, 16, 32 uA. X-axis: the time interval of stimulation (1 second between ticks).

11
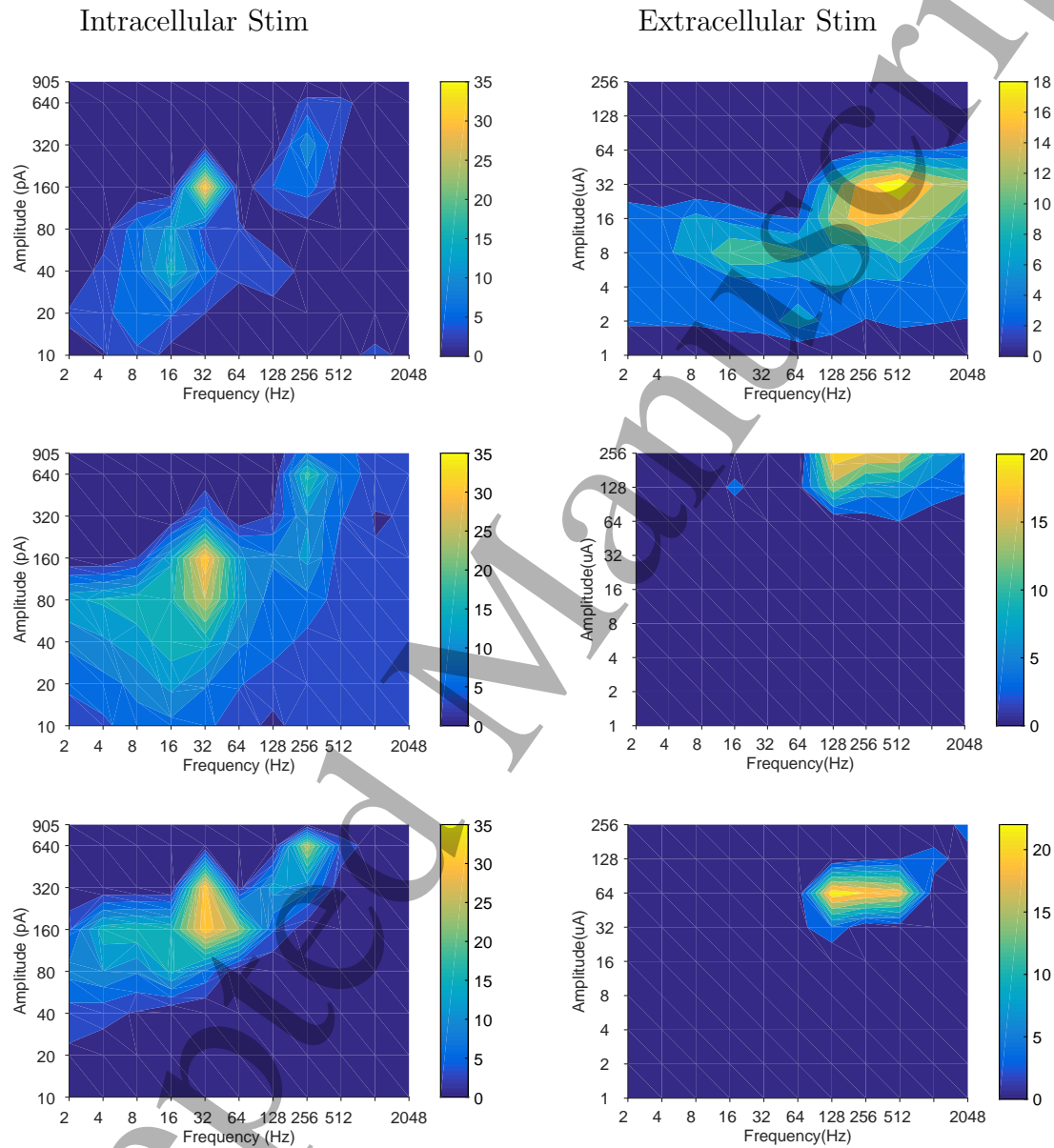
Fig. 6: Contour map showing three individual cell responses to intracellular (left column) and extracellular (right column) sinusoidal stimulation. Top row illustrates the response of the same cell as in Figure 5. Colorbars show spiking rate in response to stimulation.
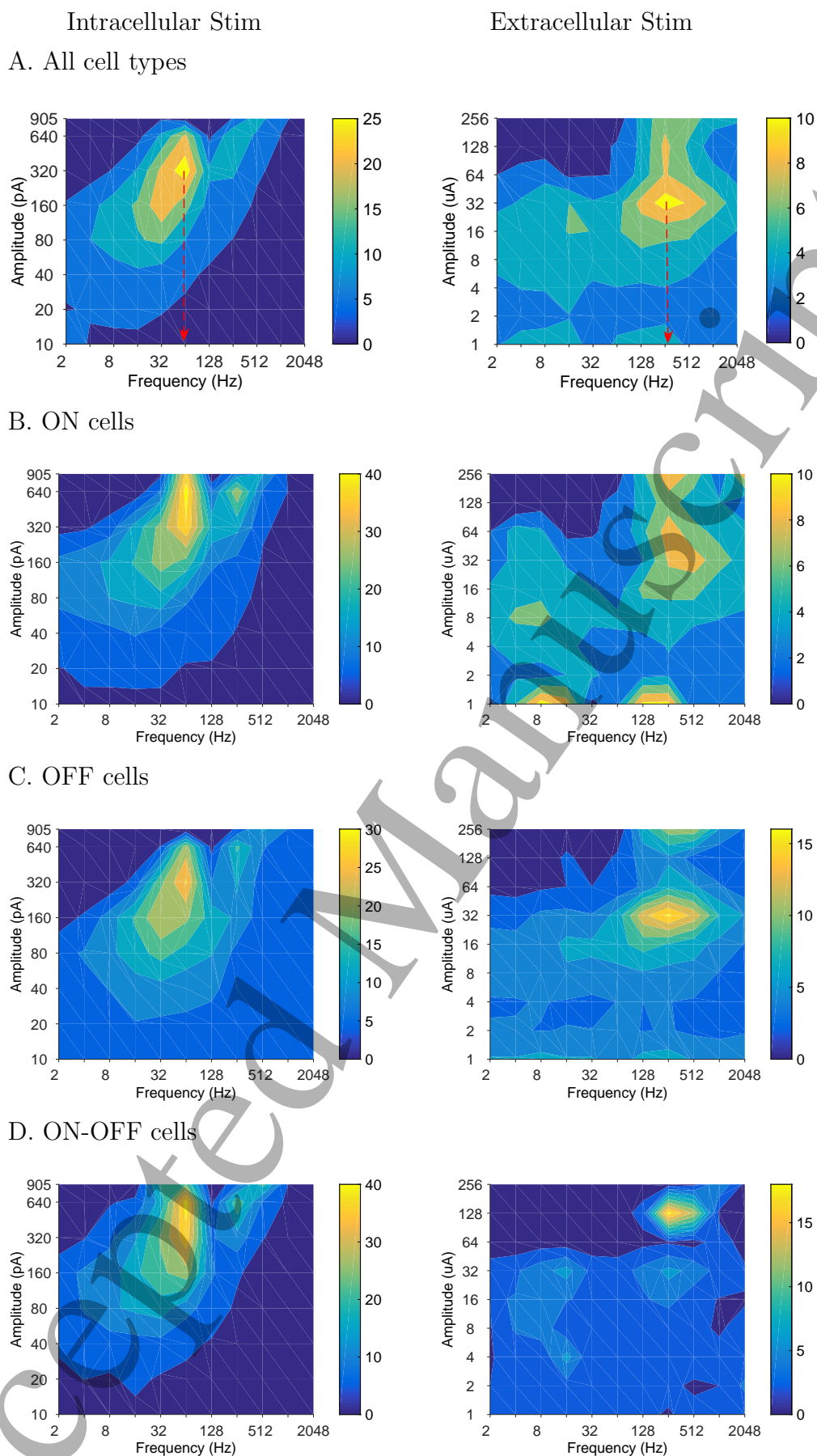
Fig. 7: Contour map showing population responses to intracellular (left column) and extracellular (right column) sinusoidal stimulation. A. Population response for all cell types. Red arrows show the stimulation frequency that leads to the maximum response. B. ON-type RGC response. C. OFF-type RGC response. D. ON-OFF-type RGC response. Colorbars show spiking rate in response to stimulation.

13

Intracellular Stim　　　　　　　　　　Extracellular Stim
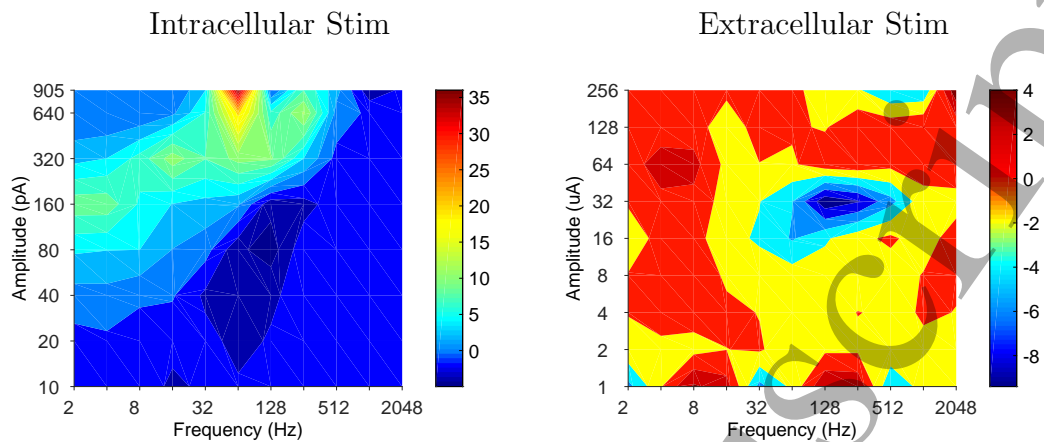
Fig. 8: Contour map showing difference between ON and OFF RGC population response to intracellular (left) and extracellular (right) sinusoidal stimulation. Colorbars show spiking rate in response to stimulation.
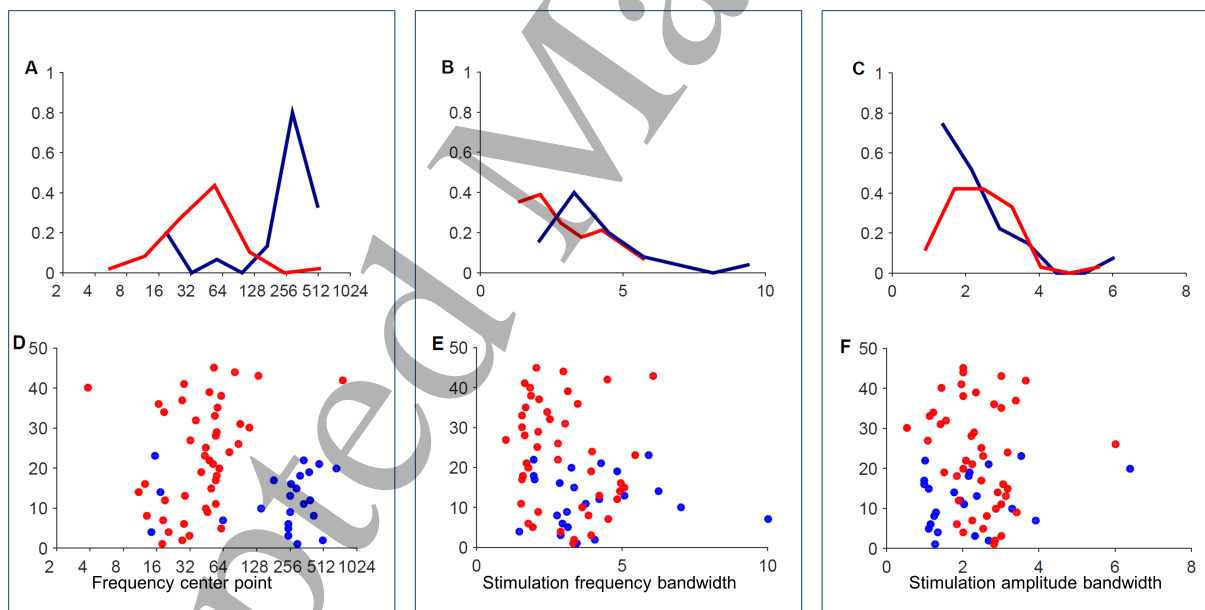
Fig. 9: Statistical analysis of the contour maps. Vertical axis on each subplot illustrates the fraction of cells in the population displaying the reported characteristics for intracellular stimulation (red) and for extracellular stimulation (blue). Horizontal axis on subplots A,D: Frequency center point; B,E: Stimulation frequency bandwidth; C,F: Stimulation amplitude bandwidth. A. Frequency center point of contour activation at half spike rate. B and C. Stimulation frequency and amplitude bandwidth of the contour activation at half spike rate, $B_F = \log_2(F_{0.5max}/F_{0.5min})$ and $B_A = \log_2(A_{0.5max}/A_{0.5min})$. D-F. The same data as in subplots A-C shown as scatter plots. Red: Intracellular stimulation; blue: Extracellular stimulation.

14

intracellular stimulation (Figure 10A), the number of spikes in response to stimulation falls as the stimulation frequency is increased. The simulated cell hardly responded to the 256 Hz stimulation and does not spike in response to 1024 Hz stimulation. The amplitude of subthreshold oscillations is smaller in the axon for higher frequencies of stimulation. This indicates that with intracellular stimulation, the axon acts as a low-pass filter, and the amplitude of high frequency components is attenuated when the signal is propagated from the soma to the axon.

Simulated membrane potentials in response to extracellular stimulation of varying frequencies are shown in Figure 10B. Contrary to the results with intracellular stimulation, when extracellular stimulation is applied, the simulated cell responds to high frequency stimulation. The amplitude of subthreshold oscillations are similar in the soma and in the axon when stimulation is applied extracellularly.

Figure 11 summarizes the data for subthreshold oscillations and spiking frequency for the voltage traces shown in Figure 10. Figure 11A illustrates the scaled amplitude of subthreshold oscillations, calculated as (abs(minV)-abs(maxV))/abs(minV). Results show that the amplitude of oscillations decreases with frequency of stimulation in the soma and in the axon, when stimulation is applied intralulularly. However, for extracellular stimulation the amplitude of subthreshold oscillations is similar for different frequencies of stimulation. Spiking frequency in response to stimulation is shown in Figure 11B. The spiking frequency in response to intracellular stimulation falls with the frequency of stimulation, while there is a peak in spiking in response to the 256 Hz extracellular stimulation. Figure 11B can be thought of as a horizontal slice for a fixed stimulation amplitude through the contour plot in Figure 7. Similar to the experimental results illustrated in Figures 6 and 7, our simulations show that the optimal extracellular stimulation frequency may be around 256 Hz (Figure 11B, red). We did not investigate the electrophysiological mechanisms leading to the maximum spiking rate at this stimulation frequency.

The axon has a low pass filtering effect on intracellular stimulation delivered at the soma, whereby high frequency signals are attenuated more rapidly along the length of the axon compared to lower frequency signals. To illustrate this, we considered the dependence of the electrotonic length constant for different frequencies of stimulation, f. The electrotonic length constant, λ, gives the scale over which spatial transients occur along the axon, so that current applied at a point on the neuron causes a depolarisation of the membrane potential along the axon that decays according to $\exp(-\lambda x)$. The electrotonic length constant is dependent on the unit length impedance of the cellular membrane inversely proportional to the stimulation frequency, as shown in [18],

$$\lambda = \lambda_0/(1 + 2\pi j\tau_m f)^{1/2} = [z_m(f)/(r_e + r_i)]^{1/2},$$

where λ_0 is the steady state value for the length constant (when $f = 0$), $\lambda_0 = [r_m/(r_e + r_i)]^{1/2}$, r_e and r_i are the resistance per unit length of the extracellular spaces and intracellular space. $j = \sqrt{-1}$, and τ_m is the membrane time constant. The frequency dependence of the electrotonic length constant arises through its dependency on the (unit length) impedance of the cellular membrane $z_m(f) = 1/[1/r_m + 2\pi jC_m f]$ which contains a capacitive component $1/2\pi jC_m f$ (as well as a resistive component of the membrane r_m). Intuitively, high frequency injected current is more easily able to pass across the

15

membrane back out into the extracellular spaces to attain the resting membrane potential because the capacitive impedance of the membrane is less at high frequency compared to low frequency.

Simulation results for the length constant values for different frequencies of stimulation are shown in Figure 12. Results show that for 2 Hz stimulation, the electrotonic length constant is 0.9. That is, if we assume that the electrical stimulation is delivered at the soma at location zero, then the spatial transients propagate to the length of 0.9 along the axon with 2 Hz stimulation. However, with the 128 Hz stimulation, the transients do not propagate far into the axon, only to the length of 0.08. The axon acts as a low pass filter, passing only the low frequency signal along the axon. If the signal reaches the axon high sodium band, a spike is initiated which is propagated further into the distal axon.

Fig.10 caption. *Simulated membrane potential in response to A. Intracellular stimulation, and B. Extracellular stimulation. The frequency of stimulation is shown at the left for each row. Column 1: Membrane potential recorded in the soma. Column 2: Membrane potential recorded in the distal axon. Stimulation amplitude: 200 pA intracellularly and 170 μA extracellularly.*

4   Conclusions and Discussion

Experimental results and simulations show that cells respond to higher frequencies during extracellular stimulation compared to intracellular stimulation. This work provides evidence that neural responses to intracellular stimulation fundamentally differ from the responses of neurons to extracellular stimulation. In particular, the optimal stimulation frequency required to elicit maximum responses is different for intracellular and extracellular stimulation. Figures 6 and 7 illustrate the existence of an upper threshold, that is, the stimulation amplitude level above which no action potentials can be elicited in electrically stimulated retina. The phenomenon of the upper threshold stimulation is discussed in detail in several papers, e.g. [4], [19], [22].

Simulations show that the cell membrane acts as a low-pass filter, explaining the difference between the responses to extracellular and intracellular stimulation. The amplitude of high frequency components of the signal is attenuated when propagated to the axon. It was shown that the electrotonic constant is inversely proportional to the square root of the spectral frequency [18]. This relationship between stimulation frequency and electrotonic time constant dictates the limit on the propagation of charge along the axon.

The electrotonic length constant predicts the extent of electric signal propagation in a neurite, estimated between 2 and 20 μm and is frequency dependent. This value is smaller than the average spread of the dendritic trees in RGCs, which range from 100 to 600 μm in rat retina [30]. Intracellular stimulation at high frequency would cause greater decay of signal propagation since stimulation is delivered only to the soma, the spread of charge may fail to reach the axon initial segment and initiate an action potential. Whilst stimulation at the soma would be able to produce depolarization of the membrane potential, which would normally produce action potentials, the threshold could not be reached at the axon initial segment. Extracellular stimulation, on the other hand, would

A. Simulations: Intracellular Stimulation
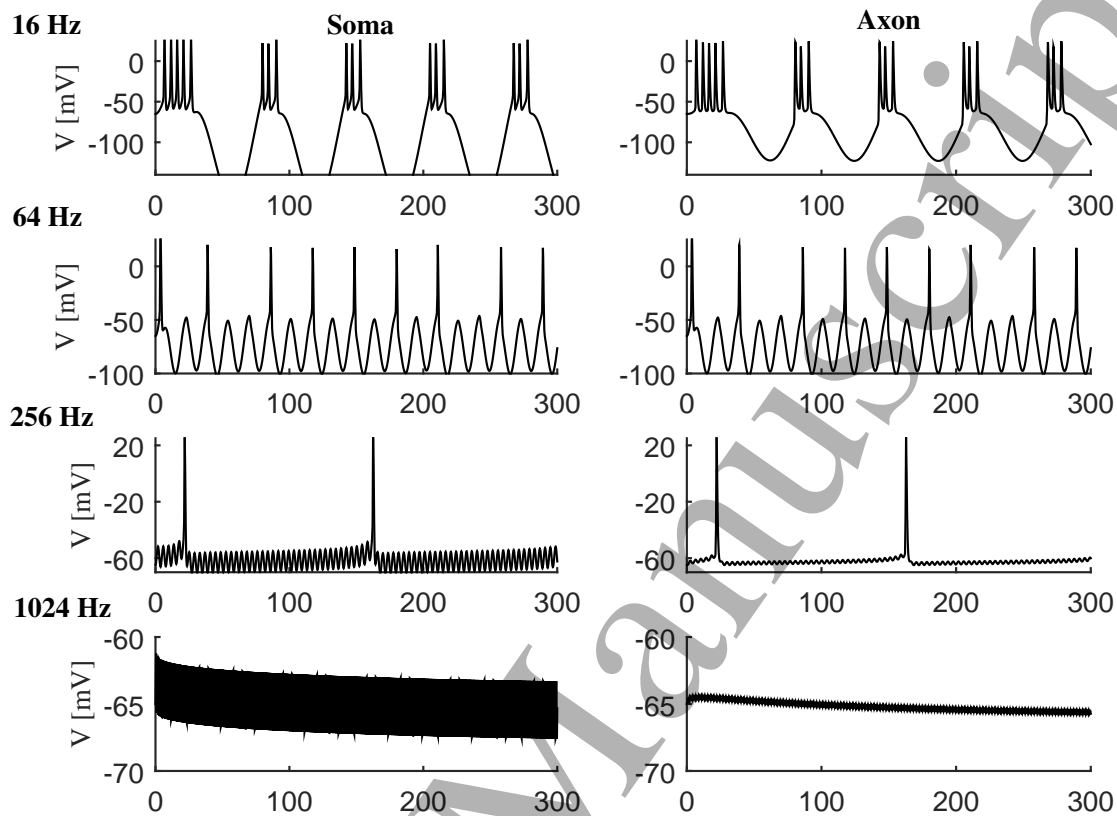
B. Simulations: Extracellular Stimulation

17
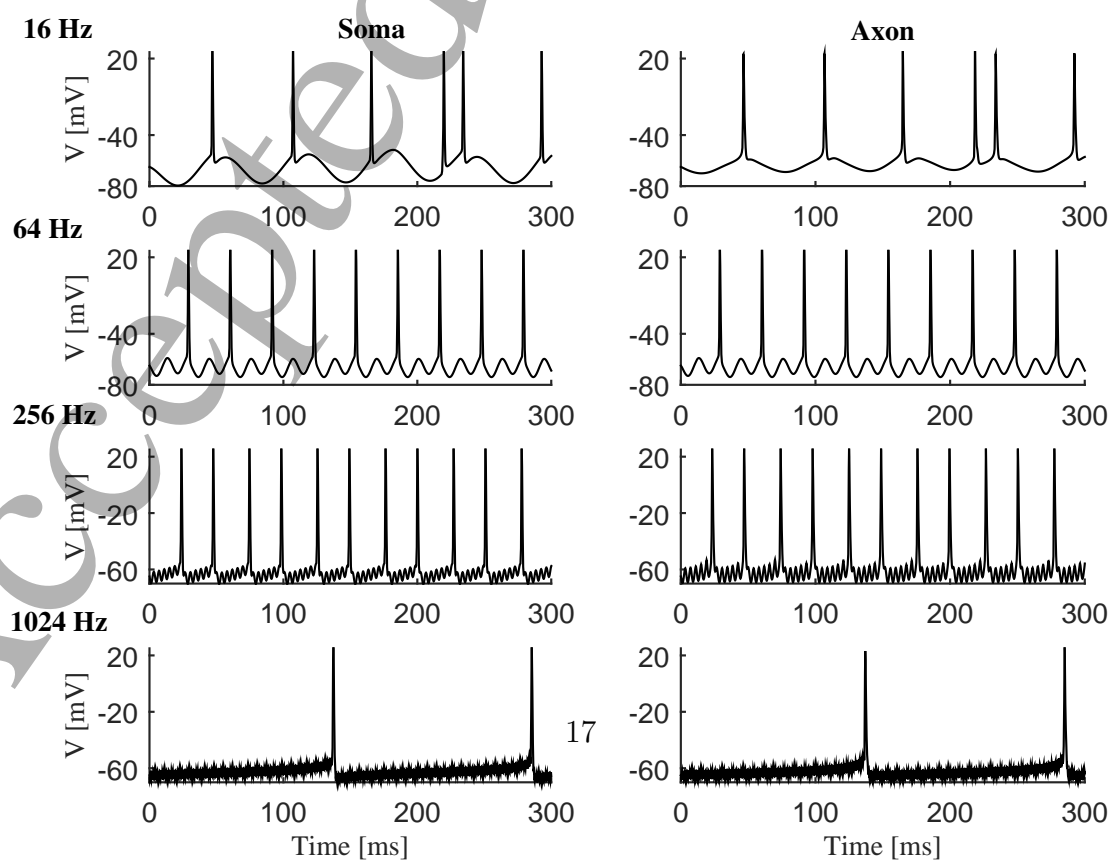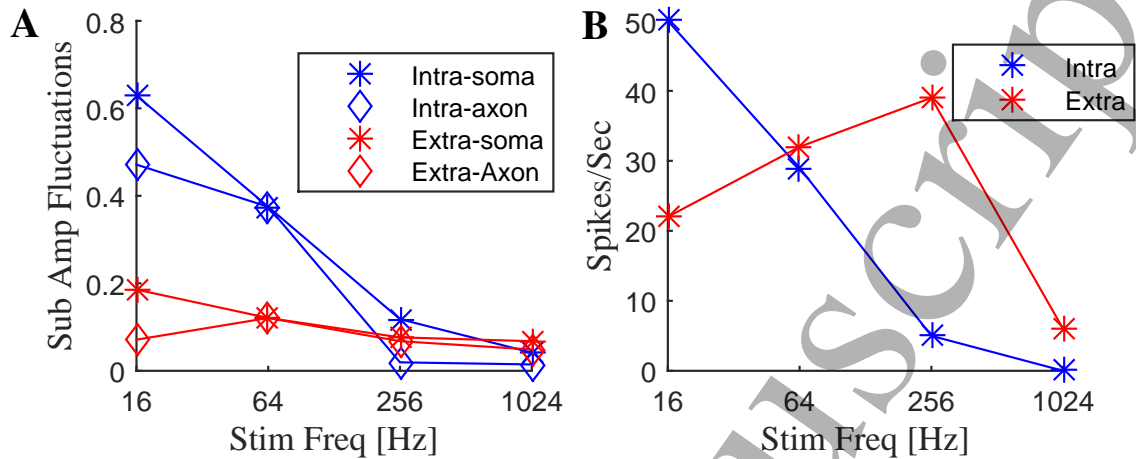
Fig. 11: Simulation results. Subthreshold oscillations and spiking frequency for voltage traces shown in Figure 10. A. Amplitude of subthreshold oscillations in the soma (stars) and in the axon (diamonds) in response to intracellular (blue) and extracellular (red) stimulation of varying frequencies. Subthreshold oscillations were calculated as follows: (abs(minV)-abs(maxV))/abs(minV). B. Number of spikes in response to intracellular (blue) and extracellular (red) stimulation of varying frequencies. Stimulation amplitude: 200 pA intracellularly and 170 μA extracellularly.
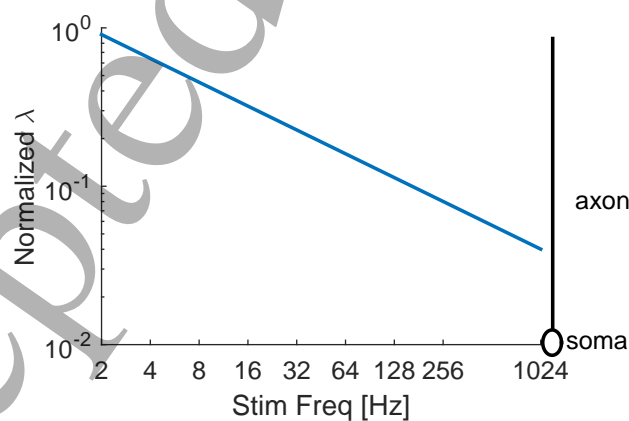
Fig. 12: The scale of the spatial transient propagation (i.e. the electrotonic length constant values) for different frequencies of stimulation (shown on log-scale). Simulation parameters: $r_m = 1e + 6$ Ω, $\tau_m = 10$ ms, $r_i = 200$ Ω, $r_e = 2000$ Ω.

18

affect the whole tissue surrounding the cell and would be able to depolarize the axon initial segment and cause initiation of a spike.

Selective activation of ON or OFF RGCs with electrical stimulation is a topic of great interest to researchers and clinicians working in the field of retinal implants. Twyford and colleagues demonstrated that ON and OFF RGCs respond differentially to high frequency biphasic stimulation [27]. The mechanisms underlying differential responses of ON and OFF cells are not proven experimentally but may be due to different ionic currents present in ON and OFF RGCs and different cell morphologies, as illustrated computationally in [13].

In our work, the ON cell population showed a narrower band of optimal stimulation than the OFF cells in the varied amplitude and frequency protocols. The physiological difference between ON and OFF cells is pronounced and well established in the retina [29]. Different activation profiles could be due to the presence of low voltage activated calcium channels in OFF cells [17]. Margolis and Detwiler found that ON cells relied on synaptic input to guide their activity, while spontaneous rates and evoked activities of OFF cells were mainly affected by intrinsic factors [16]. Mechanisms underlying the difference in activation profiles for ON and OFF cells are yet to be found. Future work should focus on revealing biochemical properties that differentiate ON and OFF cell responses.

Electrical stimulation is used to treat patients with Parkinson's disease [23], to stop seizure spread [7], and to replace lost sensory functions in patients with loss of vision and hearing [3], [8], [31]. Optimal stimulation parameters are almost always patient specific. To improve the efficacy of stimulation strategies in neuroprosthetic devices, the stimulation parameters are often tested *in vitro* using intracellular stimulation. Our work shows that one has to be cautious when translating results obtained with intracellular stimulation to those that employ extracellular stimulation.

Acknowledgments

References

[1] GA Ascoli, DE Donohue, M Halavi. NeuroMorpho.Org: a central resource for neuronal morphologies. *J Neuroscience,* 27(35): 9247-9251, 2007.

[2] AK Ahuja, JD Dorn, A Caspi, MJ McMahon, G Dagnelie, L daCruz, P Stanga, MS Humayun, RJ Greenberg. Blind subjects implanted with the Argus II retinal prosthesis are able to improve performance in a spatial-motor task. *British J Ophthalmology,* 95(4): 539 - 543, 2010.

[3] LN Ayton et al. First-in-human trial of a novel suprachoroidal retinal prosthesis. *PLoS One*, 9 e115239, 2014.

[4] D Boinagrov, S Pangratz-Fuehrer, B Suh, K Mathieson, N Naik, D Palanker. Upper threshold of extracellular neural stimulation. *J of Neurophysiology,* 108(12), 3233-323, 2012.

[5] DM Durand. Electric Stimulation of Excitable Tisue, in The Biomedical Engineering Handbook. Ed. Joseph D. Bronzino, *CRC Press LLC*, 2000.

[6] JF Fohlmeister, RF Miller. Mechanisms by which cell geometry controls repetitive impulse firing in retinal ganglion cells. *J Neurophysiology,* 78(4):1948-1964, 1997.

[7] R Fisher et al. Electrical stimulation of the anterior nucleus of thalamus for treatment of refractory epilepsy. *Epilepsia*, 51(5), 899 - 908, 2010.

[8] D Grayden, G Clark. Implant design and development, Cochlear Implants: A Practical Guide, *Whurr Publishers*, 2006.

[9] AE Hadjinicolaou, SL Cloherty, Y-S Hung, T Kameneva, MR Ibbotson. Frequency responses of rat retinal ganglion cells. *PLOS One*, 11(6): e0157676. doi:10.1371/journal.pone.0157676, 2016.

[10] OP Hamill, A Marty, E Neher, B Sakmann, FJ Sigworth. Improved patch-clamp techniques for high-resolution current recording from cells and cell-free membrane patches. *Pflgers Archiv*, 391(2), 85-100, 1981.

[11] M Hines. NEURON a program for simulation of nerve equations. *In: Neural Systems: Analysis and Modeling, edited by F. Eckman. Norwell, MA: Kluwer Academic Publishers,* 1993.

[12] LH Jepson, P Hottowy, K Mathieson, DE Gunning, W Da Browski, AM Litke, EJ Chichilnisky. Focal electrical stimulation of major ganglion cell types in the primate retina for the design of visual prostheses. *J Neuroscience,* 33(17): 7194 -7205, 2013.

[13] T Kameneva, MI Maturana, AE Hadgjinicolaou, SL Cloherty, MR Ibbotson, DB Grayden, AN Burkitt, H Meffin. (2016) Retinal ganglion cells: mechanisms underlying depolarization block and differential responses to high frequency electrical stimulation of ON and OFF cells. *J of Neural Engienering*, 13: 016017.

[14] C Koch, I Segev. Methods in neuronal modelling. *MIT Press, Cambridge*, 2001.

[15] JA Latikkal, JA Hyttinen, TA Kuume, H . Eskola, JA Malmivuo. The conductivity of brain tissues: comparison of results in vivo and in vitro measurements, *Proceedings EMBS Conference*, 910-912, 2001.

[16] DJ Margolis, PB Detwiler. Different mechanisms generate maintained activity in ON and OFF retinal ganglion cells. *J of Neuroscience*, 27(22): 5994-6005, 2007.

[17] DJ Margolis, AJ Gartland, T Euler, PB Detwiler. Dendritic calcium signaling in ON and OFF mouse retinal ganglion cells. *J of Neuroscience*, 30(21), 7127-7138, 2010.

20

[18] H Meffin, T Kameneva. The electrotonic length constant: A theoretical estimate for neuroprosthetic electrical stimulation. *Biomedical Signal Processing and Control*, 105-111, 2011.

[19] K Meng, A Fellner, F Rattay, D Ghezzi, H Meffin, MR Ibbotson, T Kameneva. Upper stimulation threshold for retinal ganglion cell activation. *J of Neural Engineering*, 2018, doi: 10.1088/1741-2552/aabb7d.

[20] PG Patil, DA Turner. The development of brainmachine interface neuroprosthetic devices, *Neurotherapeutics,* 5: 13746, 2008.

[21] F Rattay. Electrical Nerve Stimulation: Theory, Experiments and Applications. *Springer*, 1990.

[22] F Rattay. On the upper threshold phenomenon of extracellular neural stimulation. *J of Neurophysiology,* 112: 2664-2665, 2014.

[23] J Roper, N Kang, J Ben, J Cauraugh, M Okun, C Hass. Deep brain stimulation improves gait velocity in Parkinson's disease: a systematic review and meta-analysis. *J of Neurophysiology*, 263(6): 1195 - 1203, 2016.

[24] S Sekhar, A Jalligampala, E Zrenner, DL Rathbun. Tickling the retina: integration of subthreshold electrical pulses can activate retinal neurons. *J Neural Engineering,* 13 046004, 2016.

[25] W Sun, N Li, S He (2002). Large scale morphological survey of mouse retinal ganglion cells. *J of Comparative Neurology,* 451 (2): 115 - 126.

[26] HC Tuckwell. Introduction to theoretical neurobiology: volume 1 linear cable theory and dendritic structure. *Cambridge University Press,* 1988.

[27] P Twyford, C Cai, S Fried. Differential responses to high-frequency electrical stimulation in ON and OFF retinal ganglion cells. *J Neural Engineering*, 11: 025011, 2014.

[28] P Twyford, S Fried. The Retinal Response to Sinusoidal Electrical Stimulation. *IEEE Transactions on Neural Systems and Rehabilitation Engineering,* 413 - 423, 2015.

[29] H Wassle. Parallel processing in the mammalian retina. *Nature Reviews Neuroscience,* 5(10): 747-757, 2004.

[30] RC Wong, SL Cloherty, MR Ibbotson, BJ O'Brien. Intrinsic physiological properties of rat retinal ganglion cells with a comparative analysis. *J of Neurophysiology*, 108(7): 2008-2023, 2012.

[31] JD Weiland, W Liu, MS Humayun. Retinal prosthesis. *Annual Review Biomedical Engineering,* 7:361-401, 2005.